ELSEVIER

Journal of Chromatography A, 740 (1996) 169–181

JOURNAL OF CHROMATOGRAPHY A

Column radial homogeneity in high-performance liquid chromatography

Tivadar Farkas[a,b], Michael J. Sepaniak[a,b], Georges Guiochon[a,b,*]

[a]*Department of Chemistry, University of Tennessee, Knoxville, TN 37996-1600, USA*

[b]*Division of Chemical and Analytical Sciences, Oak Ridge National Laboratory, Oak Ridge, TN, USA*

Received 17 November 1995; revised 31 January 1996; accepted 2 February 1996

Abstract

The radial distribution of analyte molecules within an elution band in HPLC was determined by local, on-column, fluorescence detection at the column outlet. Several optical fiber assemblies were implanted in the exit frit at different points over the column cross-section and the fluorescence of a laser-dye analyte was measured. The individual elements of a diode array were used as independent detectors. The distribution of the mobile phase velocity across the column was measured for a number of standard size analytical HPLC columns of different efficiencies, operated at different mobile phase linear velocities. The dependence of the column efficiency on these profiles is discussed.

Keywords: Flow velocity distribution; Fluorescence detection, on-column; Column efficiency

1. Introduction

There is now incontrovertible evidence that chromatographic columns are not radially homogeneous [1–8]. Using a dual-(micro)electrode polarographic detector, Knox et al. [1] were the first to demonstrate this phenomenon, by recording the elution of a band of *p*-nitrophenol at various radial locations, at the exit of a 11.7 mm I.D. column packed with 64-μm solid glass beads. These authors reported marked differences between the local values (which are averages of contributions taking place all along the column) of the residence time and the apparent efficiency measured across the diameter of the column. These results were confirmed by Eon [2] who also showed that the variance of the values of the efficiency measured at constant radius, in eight different positions equidistant to the column center, increases with increasing value of the radius, suggesting increasing packing disorder from the center to the wall of the column. In both cases [1,2], the average mobile phase velocity and the column HETP are higher near the wall of the column than in its center.

These results had been obtained with dry-packed columns. A similar radial dependence of the HETP was obtained later with slurry-packed columns [3–5]. However, in this work, the mobile phase velocity was observed to be lower near the column wall. The difference between the flow velocity distribution in dry- and slurry-packed columns is probably related to differences in the bed structure caused by these packing procedures, as discussed later.

More recently, NMR imaging of solute bands

*Corresponding author. Address for correspondence: Department of Chemistry, University of Tennessee, 575 Buehler Mall, Knoxville, TN 37996-1600, USA.

0021-9673/96/$15.00
PII S0021-9673(96)00107-0

during their migration along chromatographic columns has shown considerable differences between the 3-D profiles recorded experimentally for these bands and the flat profiles usually assumed in theoretical discussions [6–9]. In some cases, the differences are due to flow perturbation caused by the viscosity difference between the pure mobile phase and the solution of the feed components [6]. Even when these differences are negligible, however, the bands are found to look somewhat like canvass walls in a stormy wind [8,9]. The profiles exhibit many local irregularities superimposed on a general trend which is not planar. The local thickness of the bands corresponds to values of the reduced column HETP of the order of 1.2 to 1.5, while the average value given by a bulk detector is of the order of 3 [8].

A systematic variation of the local column packing density and packing homogeneity is the simplest explanation for these results. In the case of dry-packing, the radial dependence of the packing density can be attributed to the segregation of particles by size while they slide down the heaps which form when the material is poured down the column or while radial vibrations are applied to consolidate the bed. In slurry packing, the heterogeneity of the bed originates in the differential degree of sedimentation caused by the proximity of the column wall. Both mechanisms tend to cause the packing density to have a mainly cylindrical distribution. None of them, however, and certainly not the differential degree of sedimentation of slurries, imply that the packing density be homogeneous along a straight line parallel to the column axis. Important systematic variations in the axial direction are quite possible but they are certainly much less harmful than systematic radial fluctuations. They are also, as a consequence, more difficult to detect.

Local fluctuations of the packing density cause correlative fluctuations of the local porosity, permeability and retention characteristics of a column. As a consequence, the streampaths are no longer parallel to the column axis. The average velocity of the bands along a streampath is a function of the radial position of the line. Diffusion coefficients of analytes in solutions are too low to permit a rapid relaxation of the radial concentration gradients induced by these fluctuations. Thus, in addition to the classical sources of band broadening [10], new ones have to be considered [11,12]. As a consequence, column performance is reduced: the resolution between peaks in analytical separations, or the production rate and recovery yield of the purified fractions obtained in preparative applications, respectively, are decreased [12].

In the work of previous authors [1–4], on-column local detection has been performed by placing a single miniature detector element at various points over the column cross-section. Studies aiming at mapping out the radial distribution of the analyte concentration within a chromatographic band involved single channel detection followed by reconstruction of the analyte band shape using data recorded during different runs [2–4]. This approach cannot compensate for the experimental variations in the peak height, area, shape and retention time which are usually encountered even when experimental conditions are maintained constant with special care. In our previous work [5], we performed on-column local electrochemical detection by placing four 150 μm O.D. gold microelectrodes in the column exit frit and by monitoring their output simultaneously [5]. Only a multiple channel detection method can measure accurately the differences in local analyte concentration between different sites of the eluting chromatographic band.

We wanted to extent this work to the systematic investigation of the behavior of large diameter columns used in preparative chromatography. The results of NMR imaging studies [8,9] suggest that a rather large number of local measurements would be necessary for that purpose. Because of the considerable cost of the electronic devices required to operate electrochemical detectors, it was impossible to use more than the two double units of our original work [5]. Attempts at using a multiplex approach and acquiring with a computer the signals of a larger number of electrodes failed. Furthermore, the gold microelectrodes proved to be very feeble mechanically and chemically. They broke easily and their response in time showed a fast decay. In contrast to what previous authors have reported [3,4,13–15], electrochemical cleansing was not particularly effective at regenerating the electrode surface. Replacing a microelectrode required a new calibration step and questioned at the same time the congruity in data collection within a given set of experiments.

The present work describes results similar to those

reported previously [5] but carried out on different columns, using laser induced fluorescence as the detection principle and an implementation based on the use of quartz optical fibers.

2. Experimental

The experiments described here were performed using laser dyes as the analytes. The beam of an argon ion laser is directed with optical fibers to locations of choice at the column outlet. The fluorescence signal induced by the excitation of the analyte molecules is collected by other optical fibers and carried to the appropriate pixels of a diode-array. An electrical signal proportional to the amount of light received by each pixel is acquired and stored in a computer. The only requirement for choosing an analyte was that its retention factor be small when using columns packed with conventional materials. The choice of a laser dye was largely based on high detection sensitivity. The use of optical fibers allows the easy selection of the locations where detection will be carried out. Each of the components of the system are discussed below in detail.

2.1. Optical fibers

The new experimental design consists of a number of optical fiber assemblies inserted perpendicularly into the column exit frit (Fig. 1). Such extrinsic optical sensors are widely used for fiber optic remote, in situ measurements. These sensors utilize the fiber as a means of transmitting light between the

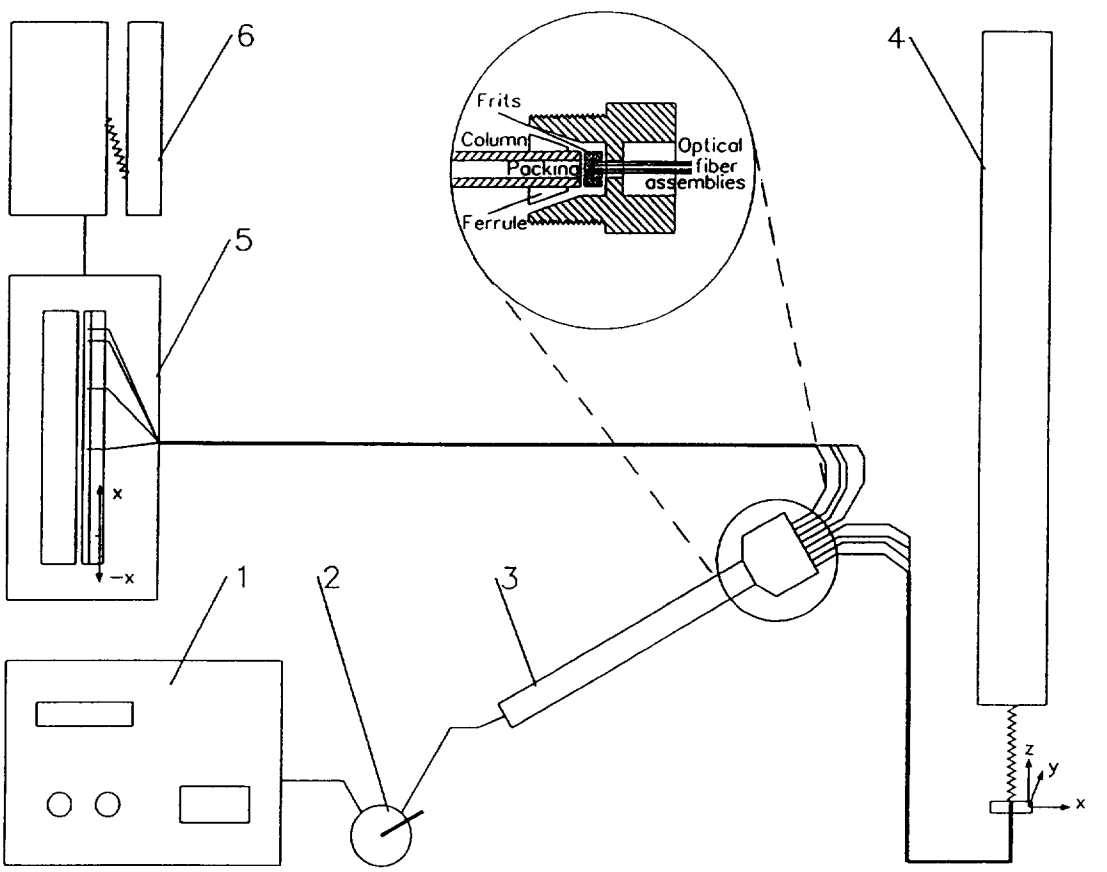

Fig. 1. Instrumental set-up for local on-column fluorescence detection using optical fibers. (1) HPLC pump; (2) injection valve; (3) chromatographic column; (4) argon ion laser; (5) photodiode array detector; (6) microcomputer. The inset shows the cup-shaped fitting with the optical fiber assemblies.

measurement instrumentation and an external transducer that is located within the sample, proximal to the opposite end of the fiber [16]. Direct sensors measure the inherent spectroscopic signals of the analyte of interest such as its absorbance or fluorescence [17,18].

In our case, each assembly contains two fibers, one of which (the excitation fiber) carries the excitation beam from the source to the investigated spot, while the other fiber (the emission fiber) collects part of the light signal emitted by fluorescence and transmits it to the detector. These assemblies allow for the on-column local photometric detection of the analyte molecules using an external diode-array as light detector.

The design of the optical fiber assemblies is illustrated in Fig. 2. The quartz fibers (General Fiber Optics, Cedar Grove, NJ, USA) have a core diameter of 105 μm and are 90 cm long. The jacket at one end of each fiber was removed to a distance of 6 to 7 mm. The uncovered quartz tips were inserted in a 5 mm long, 0.25 mm nominal I.D. stainless-steel needle-gauge tubing (Hamilton, Reno, NV, USA). This metallic sheath protects the uncovered silica cores which are very brittle and facilitates the handling of the fiber assemblies. Epoxy resin (Epon Resin 828; Shell, Houston, TX, USA) was used to seal the fibers in the tubing. The epoxy filling prevents assembly fouling by analyte deposition inside the metallic tubing and ensures the mechanical rigidity of the joint. This assembly design was meant to keep the two optical fiber tips as close as possible, such that their acceptance cones overlap to the largest extent (see Fig. 2). Such a geometry should ensure the best efficiency in collecting the fluorescent light emitted as analyte molecules pass by the fiber tips. The assembly tips are then inserted in a Delrin holder and wheel-polished with diamond paste and alumina. This step ensures the removal of excess epoxy from the assembly tips and generates fiber tips which are reasonably flat.

The initial locations of the assembly tips over the column cross-section are shown in Fig. 3. By rotating the holding frit within the modified exit fitting (see inset in Fig. 1) by one or several steps of 90° around the column axis, further locations could be investigated and data could be collected with the same assemblies along different diameters of the column cross-section. This system allows for a rather detailed mapping of the band profile at the column exit.

2.2. Optical system

The excitation source was an argon ion laser Model INNOVA 100-15 (Palo Alto, CA, USA) operated at 488 nm and an estimated power at the sensing side of the optical fibers of 700 mW. The resulting fluorescence transmitted by the emission fibers was detected and measured with an LDC

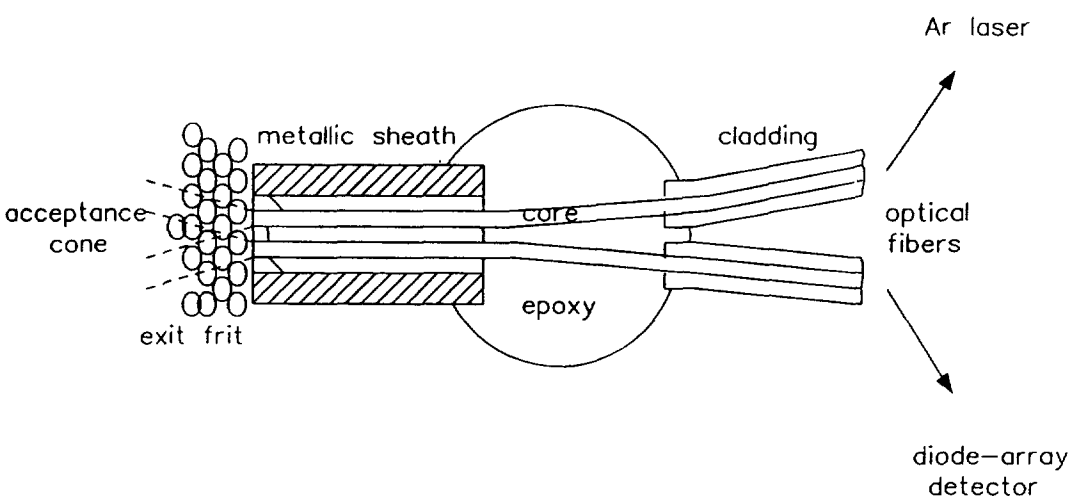

Fig. 2. Schematic of an optical fiber assembly facing the exit frit.

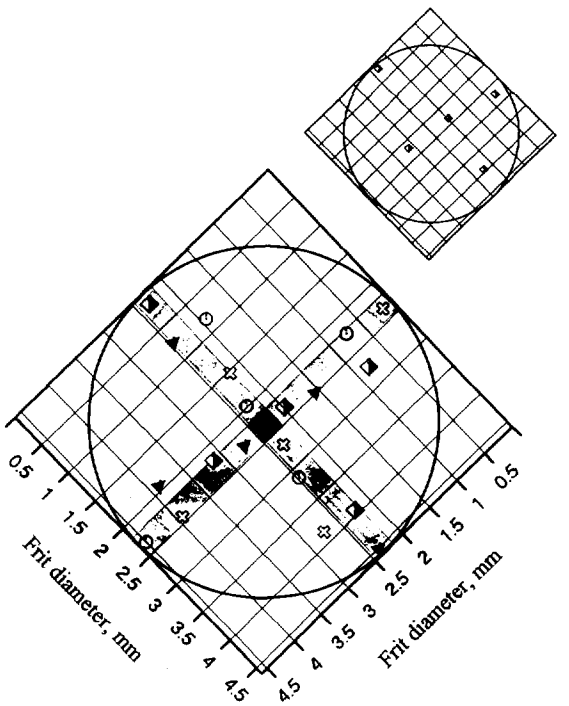

Fig. 3. Positions of the assembly tips over the column cross-section. The locations marked with a given symbol are those where the analyte concentration was monitored during a given run, for a given position of the holding frit. The insert shows the initial position of fiber tips, at 0° rotation.

(Riviera Beach, FL, USA) Analytical SpectroMonitor 5000 photodiode array detector (PDA) by scanning its elements one by one, much like individual detectors. Such an approach offers the potential of recording data on 35 parallel channels, while using a single detector unit. In practice, however, we found that only every second – or even better every third – diode element of the array could be used selectively because of optical cross-talk between adjacent elements. This still allows simultaneous detection on more than ten parallel channels, although only five were used in this work.

The diffraction grating unit of the PDA was replaced with a metallic holder which kept the emission fiber tips perpendicular and very close to the diode-array surface. The horizontal position of this holder could be adjusted such that each fiber tip be centered on one single diode. Nevertheless, cross-talk between neighboring diodes was registered, partly because dispersion took place at unevenly cleaved fiber tips, and also probably because the collected light was somewhat dispersed in the plastic filter layer (see below) that separated the fiber tips from the diode-array. Since at the miniature scale of the detector elements there was no room for a monochromator or line filter to be placed in front of each diode, we placed a thin colored plastic film (Edmund Scientific, Barrington, NJ, USA) between the fiber tips and the diode array. This cuton filter (#809 STRAW; 50% of maximum transmission at 530 nm) reduced considerably the high background signal caused by scattered excitation light.

2.3. Liquid chromatography system

The chromatographic system consisted of a Beckman (Fullerton, CA, USA) HPLC Pump Model 110B, a Rheodyne (Cotati, CA, USA) injection valve Model 7010, the LDC photodiode array detector (see previous section), and a Spectraflow (Applied Biosystems, Ramsey, NJ, USA) absorbance detector Model 575 as a bulk detector when needed. The analog output of the PDA was recorded by running a program written on an IBM ValuePoint PC [19]. The data of the UV detector were acquired using a Waters system interface module (Waters Maxima 820 version 3.3 software, Milford, MA, USA) operated at a rate of 10 data points per second. The data files were uploaded to one of the computers of The University of Tennessee Computer Center for further calculations.

2.4. Samples

Due to their high molar absorptivity and large fluorescence quantum yields, laser dyes are excellent candidate chemicals for our measurements, although elution problems can be foreseen because of their large molecular weight and polarizability. An unretained or a weakly retained compound was needed since the primary effects of the phenomenon studied here (i.e., the degree of homogeneity of the packing density) is hydrodynamic in nature. Mobile phase optimization could overcome the problems related to an excessively large retention factor. After several tentative runs made with different dyes (searching for optimum capacity factor and peak shape) three

potential analytes were selected for a more detailed investigation:

1. Fluorescein (3′,6′-dihydroxyspiro[isobenzofuran-1(3H),9′-[9*H*]xanthen]-]-one),
2. Disodium Fluorescein (disodium salt of the previous compound) and
3. Pyrromethene 556 (disodium-1,2,5,6,8-pentamethylpyrromethene-2,6-disulfonate-difluoroborate),

all products of Exciton (Dayton, OH, USA). The retention times and band profiles of the first two dyes proved to be too susceptible to pH changes and showed poor peak shape reproducibility. The use of a buffered mobile phase did not help solve this problem.

Pyrromethene (PM) showed consistently good peak shapes, and a fairly high detector response due to its high molar absorptivity, $\epsilon_{488}=6.4\times10^4$ l mol^{-1} cm^{-1}, and its good quantum yield ($\Phi_f=0.73$ in water). In order to be consistent with our previous work [5], we used a 40% methanol–60% water mixture as the mobile phase and reversed-phase adsorbents as the stationary phase. The electrolyte used in the prior work (KCl, required by the electrochemical detection method) was replaced by borax (at a concentration of 5×10^{-3} *M*) needed as a buffer that ensured good peak shape reproducibility. The concentration and volume of the injected PM samples were approximately 8×10^{-4} *M* and 20 μl, respectively.

2.5. Injection profile

A detailed discussion of the injection profile achieved with our set-up has been given previously [5]. This is important because the design of the column inlet could make much difference in the linear velocity distribution over the cross-section at the column inlet. As reported previously, when the chromatographic column is removed and the on-column detection system is attached directly to the inlet fitting of the column, we found little difference between the retention times and the variances of the peaks recorded at any point over the column cross-section, indicating a flat distribution at the column inlet.

2.6. Chromatographic columns

Standard 4.6 mm I.D. HPLC columns were investigated. Different commercially available packing materials were used for packing these columns such as: Kromasil (EKA Nobel, Surte, Sweden), a spherical particle, C_8 and C_{18} bonded silica, 16 μm average size; Zorbax (BTR Separations, Wilmington, DE, USA), a spherical particle, C_{18} bonded silica, 10 μm average size; and Bondapack H (Waters) a C_{18} bonded silica, 37–55 μm average particle size. Column lengths varied between 100 and 250 mm.

Columns were slurry packed under a final pressure ranging between 420 and 550 atm, depending on manufacturer specifications. The slurry was obtained by suspending 2–3 g of packing material in 30 ml methanol by ultrasonication for 3 min. This slurry was pushed through the column by 200 ml of methanol, pumped under maximum packing pressure for bed stabilization. All columns were tested in a conventional HPLC chromatographic instrument consisting of a Waters pump, a Rheodyne injection valve and a UV-Vis absorbance detector (Applied Biosystems). The analytes used, uracil and PM, are unretained in the buffered methanol–water mobile phase.

3. Results and discussion

Frontal analysis experiments were run for each set-up of optical fiber assemblies. The advantage of frontal analysis over elution for these studies is that, even if the packing is heterogeneous, the composition of the whole effluent becomes eventually homogeneous, given enough run time. Recalibration of the relative responses of each of the optical fibers assemblies is performed prior to each experiment. The ratio of the steady-state signal heights measured at different locations over the column cross-section to the signal at column center was used as a calibration correction factor.

Indeed, there are several reasons for which responses recorded during one run at different locations are different. Firstly, the light intensity imping-

ing on the excitation fibers varied depending on their location within the laser beam. The power output of the laser exhibited a gaussian intensity distribution around its axis. The farther an optical fiber tip is placed from the beam axis, the less light it collects. The optimal situation is when all tips are placed concentrically and closely around the beam axis. Such an alignment proved difficult to accurately accomplish. Secondly, due to the manner in which the fibers were cleaved and inserted into the column frit, laser backscatter varied between assemblies. Another important factor that determines the assembly response is its geometry. As stated before, the more the acceptance cones of the two fibers within an assembly interfere, the better the fluorescence collection yield. The degree of overlap of these cones depends much on the lateral distance between the two fibers. Finally, the different elements of the diode array do not show the same sensitivity.

Normalized frontal analysis breakthrough curves exhibit a retention time and a slope which depend on the location of the measurement. The curve having the steepest slope was also the one to elute the first. It is located around $r_c/3$ away from the column axis. It is not eluted much earlier nor is it much steeper than the breakthrough curve recorded on the column axis (Fig. 4a). The slowest and less steep breakthrough curve was recorded at the column wall (Fig. 4b). This observation seems to suggest that the packing density is higher at the column wall since the mobile phase flow velocity is slowest there.

All columns studied were tested in a conventional HPLC chromatographic system specified before, using unretained analytes like uracil and PM dis-

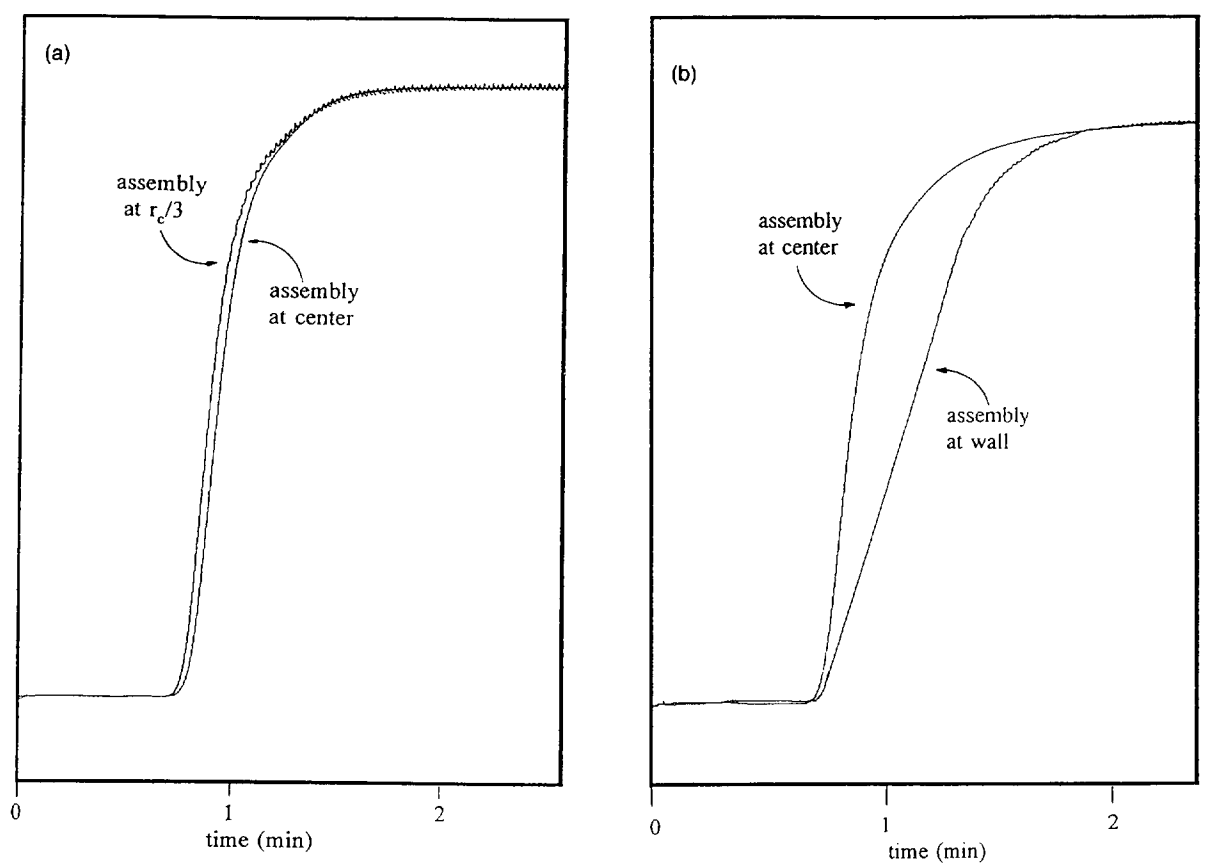

Fig. 4. Normalized break-through curves recorded during the same run at: (a) the column center and a point located at $r_c/3$ away from the column axis; (b) the column center and a point close to the column wall. HPLC column Kromasil KR100-16-C_{18} 150×4.6 mm; particle size 16 μm.

solved in the mobile phase described before. Van Deemter plots for a 100×4.6 mm column packed with Zorbax PRO-10/150 C_{18} spherical silica are presented in Fig. 5. The apparent efficiency depended strongly on the analyte of choice. The column reduced plate height was much higher for PM than that for uracil at all commonly used flow-rates (0.1–1.0 ml/min). Two parameters seem to be responsible for this phenomenon. Firstly, the diffusion coefficients for these two analytes must be very different. According to the Wilke and Chang [20] correlation between D_m and the experimental parameters, the calculated value is 2.69×10^{-6} cm^2/s for PM, versus 6.32×10^{-6} cm^2/s for uracil. Secondly, the corrected retention time for PM on this column at a flow-rate of 1 ml/min was 16% shorter than for uracil. Since uracil is unretained on ODS columns, the total accessible column volume experienced by PM seems to be significantly smaller than that for uracil. We compared the difference in elution volume for these two analytes with the total internal pore volume of the column [21], and found that their ratio was 0.76. This result suggests that PM is being excluded from most of the column total pore volume. It is improbable that PM be excluded based on its molecular size since its molecular mass is reasonably small (M_r 466.19 versus M_r=112.09 for uracil) and the bulk of its structure is given by three condensed aromatic rings (it has a rather compact structure). More probably, PM is being excluded mostly because of repulsion that takes place between the nonpolar coating of the pore walls and ionic species (PM is the disodium salt of a disulfonic acid) dissolved in an aqueous phase [22]. Nevertheless, the ionic volume of PM may be also a factor if we consider the extra contribution of its hydration sphere. The supposition that PM is being excluded from the C_{18} surface will also explain why the dependence of the reduced HETP for PM on the mobile phase velocity is so limited (Fig. 5). Given the poor behavior of PM on ODS columns, the efficiency determined for uracil will be considered in this paper.

Most of the columns studied in this work exhibited poor efficiency. Large changes in the mobile phase linear velocity were observed along any diameter, and the shape of the surface that represents the radial distribution of the length-averaged mobile phase

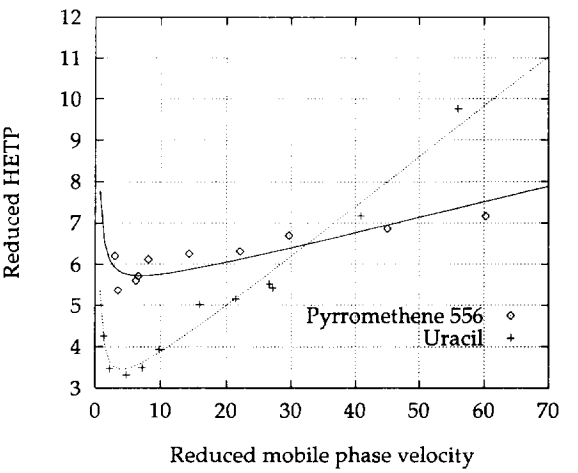

Fig. 5. Van Deemter plot for a 100×4.6 mm column packed with Zorbax PRO10/150 C_{18} spherical silica; particle size 10 μm.

velocity (calculated as the ratio of the column length and the local retention time of the breakthrough curve) was neither flat nor cylindrical. These radial profiles depend on the orientation of the diameter. A plot of the relative difference, $\Delta u/u_c$, between the linear velocity at different radial positions over the column cross-section and the velocity at the center of the column, u_c, is shown in Fig. 6. This plot is typical of poor columns with $H>100$ μm. The difference between the largest and the slowest ve-

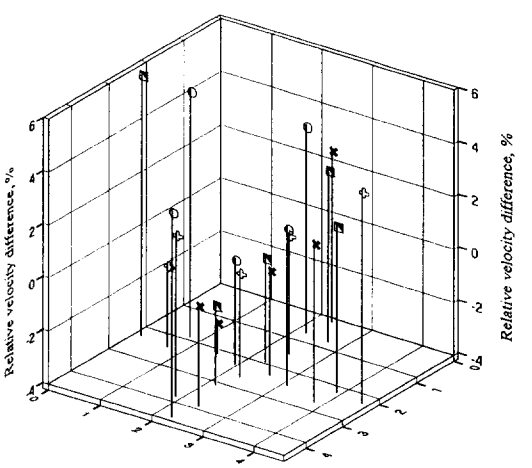

Fig. 6. 3-D view of the mobile phase velocity distribution for a Kromasil KR100-16 C_{18} HPLC column; particle size 16 μm; column dimensions 150×4.6 mm. Mobile phase: 5×10^{-3} *M* borax buffer in 40% methanol–60% water at 1.0 ml/min.

locities measured for this column was as high as 10%. We attribute this phenomenon entirely to the nonhomogeneity of the column packing because extracolumn effects are negligible with our experimental set-up. As shown previously (see Section 2), the injection profile is flat [5]. Furthermore, on-column detection precludes any postcolumn deformation of the velocity profile or extra-column band broadening.

A plot of the linear velocity versus the radius would be misleading in the present case since the velocity distribution is not symmetrical. Fig. 7a and Fig. 7b illustrate this phenomenon by showing 3-D plots of the local mobile phase velocity along the two perpendicular diameters indicated in Fig. 3.

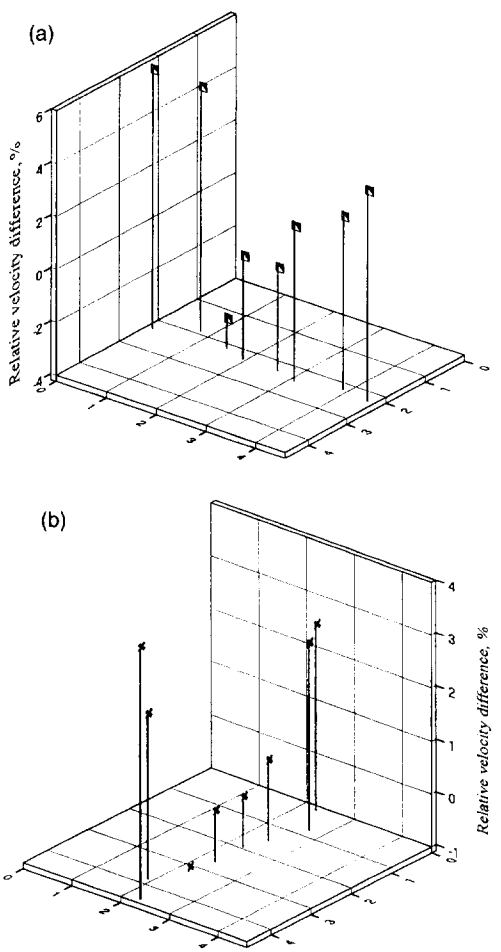

Fig. 7. 3-D view of the flow velocity along the two diameters considered in this work. Same data as in Fig. 5.

These plots demonstrate large fluctuations of the mobile phase linear velocity from one side of the column to the other and a poor radial symmetry of the velocity distribution. Overlaid 2-D plots of these two profiles (Fig. 8) show that the trends of the linear velocity along the two diameters considered are somewhat similar and correlated, although their overlap is poor. Both profiles show similar gaps on one side of the column, in vicinal regions.

By contrast, for columns having a reasonable efficiency, with $H<40$ μm, the flow profile follows mostly the pattern found in our previous work [5] and in previous reports studying highly efficient columns [3,4][1]. These results are illustrated in Fig. 9. The region of maximum velocity is. usually located at about 1/3 to 1/2 column radius off the column center. The velocity at the column center lags behind the one in this annular region by 1–2%. The velocity close to the column wall is 2–3% smaller than that at the column center.

One important difference arises, however, with the results previously reported by Baur and co-workers [3,4]. The linear velocity of the mobile phase seems to be slightly larger (at least at some radial locations) at the very column wall than in the region situated immediately next to it, a few particle diameters away

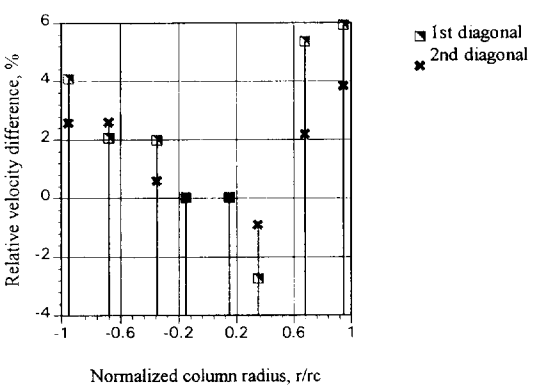

Fig. 8. Overlaid 2-D profiles recorded along two perpendicular diameters (Kromasil column as in Fig. 5).

[1]These authors used a 10 cm long column packed with an unidentified C_{18} silica (3 μm particle size), a water–methanol (90:10) buffer as the mobile phase and norepinephrine as the sample. They obtained a reduced HETP of ca. 5 at the column center and 30 near the wall.

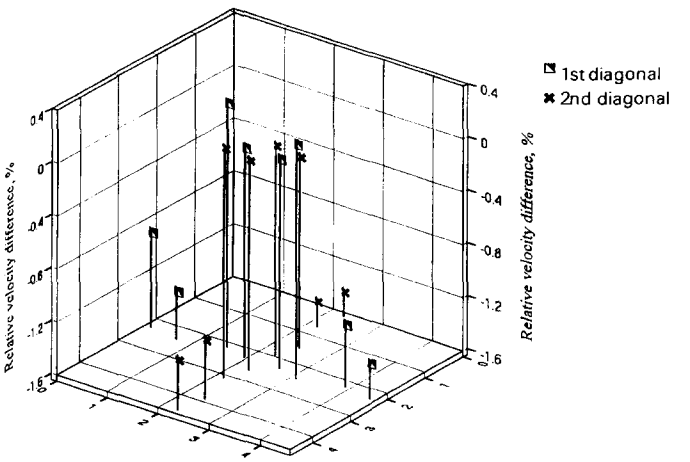

Fig. 9. 3-D view of the flow velocity distribution for an HPLC column packed with Zorbax PRO-10/150 C_{18} spherical silica; 10 μm particle size; column dimensions 100×4.6 mm.

from the column wall. This can be seen in Fig. 9, obtained with the column operated at a flow-rate of 1 ml/min. Overlaid plots of the flow profiles measured along two perpendicular diameters show a very good agreement and a reasonable degree of radial symmetry for the velocity distribution in this column (Fig. 10). A plot of the relative standard deviation (R.S.D.) of the relative velocity difference calculated from eight data points collected at locations situated on the same circle of normalized radius r/r_c but 45° apart (Fig. 11), shows that the velocity distribution in this column is cylindrical to a good approximation in the center core region (R.S.D.=6% at $r/r_c=1/3$) but that its radial fluctuations increase rapidly close to the wall (R.S.D.=20% at $r/r_c=0.95$). This observation can be explained by assuming a homogeneous packing density in the center core of the column and increasingly wide fluctuations of the local packing density close to the wall. This is consistent with results previously reported by Eon [2].

All previous investigations of the radial dependence of flow velocity have been carried out at one single value of the flow-rate [1–5]. Obviously, if the packing is heterogeneous and the local permeability

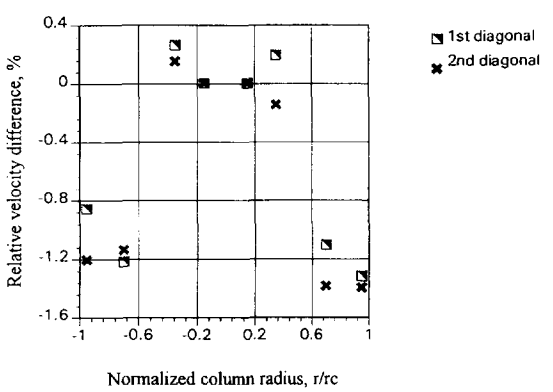

Fig. 10. Overlaid 2-D flow profiles measured along two perpendicular diameters (Zorbax column as in Fig. 9).

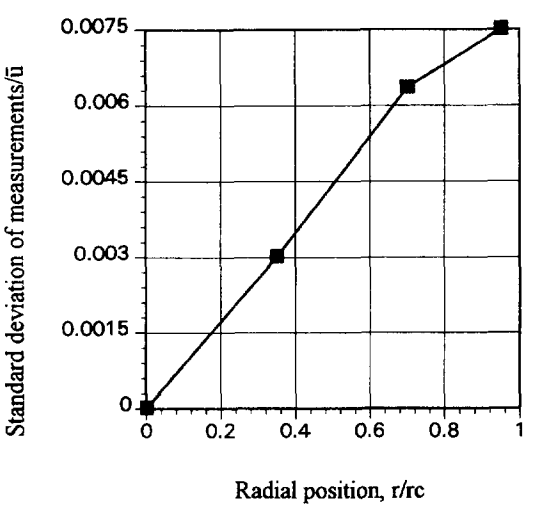

Fig. 11. Plot of the relative standard deviation of eight measurements of the mobile phase velocity performed at points located on the same circle of radius r/r_c, and 45° apart (same column as in Figs. 9,10).

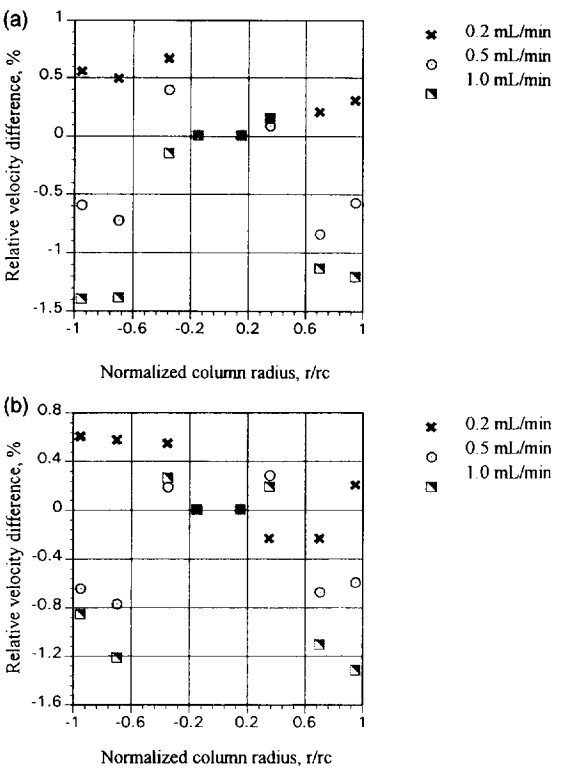

Fig. 12. Flow profiles measured at three different flow rates along a column diameter. (a) First diameter, chosen arbitrarily. Data overlaid. (b) Second diameter, perpendicular to the first one (a). Data overlaid. (same column as in Figs. 9–11).

of the column varies along its cross section, the relative values of the differences between the velocity in any location and in the center should remain constant when the flow-rate is changed, since the permeability is a property of the packing itself. Fig. 12 shows that the phenomenon is more complex than expected. As the mobile phase flow-rate decreases, the relative differences between the velocity at the center and the other local values of the velocity, which should remain constant within the limits of experimental errors, decrease significantly. The average values of these measurements and their precision (given as their standard deviations) are presented in Table 1. Admittedly, as the relative differences in local linear velocity become smaller, the precision of these measurements becomes lower. Still, the contraction of the overall elution band with decreasing flow-rate is significant.

At a flow-rate of 0.5 ml/min the relative difference in linear velocity between the fastest and the slowest regions of the flow profile was of the order of 1%, about half smaller than the value observed for a flow-rate of 1 ml/min. These relative differences became even smaller and practically negligible when the column was operated at a flow-rate of 0.2 ml/min, close to the optimum value for minimum HETP (0.1 ml/min in the present case). As seen in Fig. 12a and Fig. 12b, the profiles of the relative differences between values of the mobile phase velocity in the center of the column and at different radial positions measured along two perpendicular diameter are close. The width of these profiles (i.e., the length of their projection on the ordinate axis) increases with increasing mobile phase flow-rate. Since the width of the peak recorded by a bulk detector is related to the width of this velocity profile, the apparent column HETP should increase much faster than the local HETP. However, this increase is limited by another feature of the analyte band. We have shown in our

Table 1
Dependence of the average mobile phase linear velocity difference on fiber tip position and mobile phase flow-rate

Flow-rate (ml/min)	r/r_c					
	−0.95	−0.70	−0.35	0.35	0.70	0.95
1.0	−1.40 (0.18)	−1.39 (0.15)	−0.14 (0.18)	0.15 (0.27)	−1.14 (0.25)	−1.21 (0.15)
0.5	−0.60 (0.19)	−0.73 (0.30)	0.39 (0.13)	0.08 (0.12)	−0.85 (0.27)	−0.58 (0.11)
0.2	0.55 (0.28)	0.49 (0.22)	0.66 (0.35)	0.15 (0.18)	−0.20 (0.29)	0.30 (0.31)

Average value of 6–7 measurements; value of standard deviation given in brackets. This data is being plotted in Fig. 12a.

previous work [5] that the distribution of the analyte concentration over the column cross-section area is not flat. The concentration is higher at the column center than along the wall, in spite of the fact that the injection profile appears to be reasonably flat itself. Consequently, the flanks of the flow profile (i.e., its sides, close to the column wall) may contribute mainly to peak tailing and less to overall band broadening (only the latter translates necessarily into a plate height increase or an efficiency decrease). This explanation would be in agreement with the observation that the segments of the analyte band sampled close to column wall are diffuse. The peaks recorded along the wall are broad, with low maximum concentrations (although the signal to noise ratio is large enough to preclude a possible detection artefact).

The column efficiency calculated from the band width at half height for peaks of PM recorded at different radial locations is plotted in Fig. 13. It proves to be much lower at and close to the column wall than it is in the central region of the packing. Higher packing heterogeneity at column walls results in more important dispersion of the analyte bands and poor local efficiency. At elution from the column into a bulk detector, the already diffuse cylindrical sector of the analyte band close to the wall is being diluted even more by the centripetal flow from the core region of the eluting plug, so its effect on the overall shape of the peak profile becomes relatively minor.

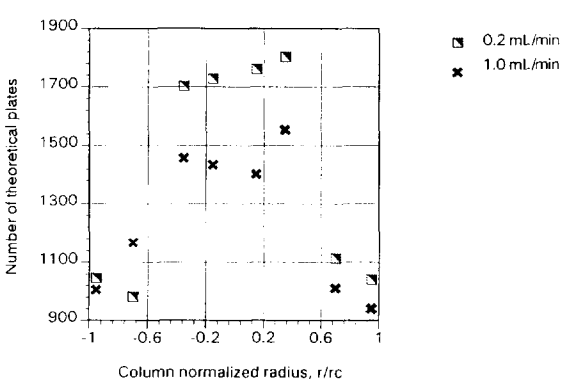

Fig. 13. Column efficiency versus radial position calculated from peak width at half height (same column as Figs. 9–12).

4. Conclusions

The new experimental set-up can accommodate at least 10 optical fiber assemblies implanted in the exit frit of an HPLC column. This number would probably be excessive to map the distribution of concentration within a chromatographic band eluting from an analytical-scale column. However, this experimental approach is most suitable for the investigation of the radial distribution of the properties of large diameter columns. Further studies regarding columns with diameters ranging from 1.25 to 5 cm in diameter are in progress.

The results reported here regarding the radial distribution of flow velocity at the outlet of an analytical column are mostly expected, since they confirm previous findings regarding columns with moderate efficiencies [1–5]. The flow distributions in these columns are cylindrical. The profiles are nearly flat in the column center (within approximately half the column radius from the center) and fall rather rapidly towards the wall. The fact that the flow distribution is not cylindrical in poor columns is new but not surprising. However, the dependence of the relative distribution of the variation of this profile on the mobile phase flow-rate is both unexpected and difficult to explain within the framework of our current concepts regarding the packing of chromatographic columns. Further investigations are required to understand this phenomenon.

Acknowledgments

This work has been supported in part by Grant DE-FGO5-88ER13859 of the Department of Energy and by the cooperative agreement between the University of Tennessee and the Oak Ridge National Laboratory. We acknowledge the contribution of Tracy Staller who wrote the data acquisition program.

References

[1] J.H. Knox, G.R. Laird and P.A. Raven, J. Chromatogr., 122 (1976) 129.
[2] C.H. Eon, J. Chromatogr., 149 (1978) 29.

[3] J.E. Baur, E.W. Kristensen and R.M. Wightman, Anal. Chem., 60 (1988) 2334.
[4] J.E. Baur and R.M. Wightman, J. Chromatogr., 482 (1989) 65.
[5] T. Farkas, J.Q. Chambers, G.A. Guiochon, J. Chromatogr. A, 679 (1994) 231.
[6] E.J. Fernandez, C.A. Grotegut, G.W. Braun, K.J. Kirshner, J.R. Staudaher, M.L. Dickson and V.L. Fernandez, Phys. Fluids, 7 (1995) 468.
[7] E. Bayer, W. Müller, M. Ilg and K. Albert, Angew. Chem. Int. Ed., 28 (1989) 1029.
[8] U. Tallarek, E. Baumeister, K. Albert, E. Bayer and G. Guiochon, J. Chromatogr. A, 696 (1995) 1.
[9] E. Bayer, E. Baumeister, U. Tallarek, K. Albert and G. Guiochon, J. Chromatogr. A, 704 (1995) 37.
[10] G. Guiochon, S.G. Shirazi and A.M. Katti, Fundamentals of Preparative and Nonlinear Chromatography, Academic Press, Boston, MA, 1994, Chapter VI.
[11] T. Yun and G. Guiochon, J. Chromatogr. A, 672 (1994) 1.
[12] T. Yun and G. Guiochon, J. Chromatogr. A, 734 (1996) 97.
[13] M. Krejči, D. Kouřilová and R. Vespalec, J. Chromatogr., 219 (1981) 61.
[14] L.A. Knecht, E.J. Guthrie and J.W. Jorgenson, Anal. Chem., 56 (1984) 479.
[15] R.L.St. Claire and J.W. Jorgenson, J. Chromatogr. Sci., 23 (1985) 186.
[16] M.J. Sepaniak, B.J. Tromberg and T. Vo-Dinh, Progr. Anal. Spectrosc., 11 (1988) 481.
[17] J.T. Coleman, J.F. Eastham and M.J. Sepaniak, Anal. Chem., 56 (1984) 2246.
[18] M.J. Sepaniak, Clin. Chem., 31 (1985) 671.
[19] T. Staller, PhD Dissertation, The University of Tennessee, Knoxville, TN, 1994.
[20] C.R. Wilke and P. Chang, AIChE J., 1 (1955) 264.
[21] H. Guan and G. Guiochon, J. Chromatogr. A, 731 (1996) 27.
[22] A. Tilly-Melin, Y. Askemark, K.-G. Wahlund and G. Schill, Anal. Chem., 51 (1979) 976.